Isolated Spin Pairs and Two-Dimensional Magnetism in $SrCr_{9p}Ga_{12-9p}O_{19}$

S.-H. Lee,[1,*] C. Broholm,[1,2] G. Aeppli,[3] T. G. Perring,[4] B. Hessen,[5] and A. Taylor[4]

[1]*Department of Physics and Astronomy, The Johns Hopkins University, Baltimore, Maryland 21218*
[2]*National Institute of Standards and Technology, Gaithersburg, Maryland 20899*
[3]*NEC, 4 Independence Way, Princeton, New Jersey 08540*
[4]*ISIS Facility, Rutherford Appleton Laboratory, Chilton, Didcot, Oxon OX11 0QX, United Kingdom*
[5]*Royal Dutch Shell Laboratories, P.O. Box 3003, 1003 AA Amsterdam, The Netherlands*
(Received 5 February 1996)

We show by inelastic neutron scattering that the frustrated magnet $SrCr_{9p}Ga_{12-9p}O_{19}$ [$p = 0.92(5)$] has dispersionless magnetic excitations at energies 18.6(1) and 37.2(5) meV. The wave vector and temperature dependence of the excitations as well as the ratio 1:2 of excitation energies is perfectly accounted for by isolated antiferromagnetically exchange coupled pairs of spins $s = 3/2$. Consideration of the layered structure of magnetic chromium ions and the ligand environment indicates that these pairs are adjacent spins in neighboring triangular lattice planes which separate two-dimensional sublattices of interacting kagomé-triangle-kagomé layers. [S0031-9007(96)00346-8]

Since its discovery in 1988 [1], $SrCr_{9p}Ga_{12-9p}O_{19}$ [SCGO(p)] has attracted a great deal of experimental [1–6] and theoretical [7] interest because of its unusual frustrated magnetism. Bulk susceptibility measurements on $p \approx 0.9$ samples [1,2] reveal antiferromagnetic (AFM) interactions (Curie-Weiss temperature $= -515$ K) which are incapable of inducing static spin correlations until a spin-glass-like transition at $T_g \approx 3.4$ K. The spin-glass state is unusual in that the specific heat is quadratic in temperature (T) at low T in contrast to the linear T dependence in ordinary spin glasses [2]. Neutron scattering experiments show the absence of long range order down to 70 mK [3,6], and an unusual extinction of elastic scattering as momentum transfer Q approaches zero [6].

It is believed that frustration in SCGO(p) is associated with two-dimensional kagomé lattices of antiferromagnetically interacting Cr^{3+} ions [1,2]. However, a complete understanding of the magnetic interactions in SCGO(p) has not been achieved, since the crystal structure is complicated and contains Cr^{3+} ions on non-kagomé planes. In this paper we report neutron scattering experiments on polycrystalline SCGO($p = 0.92(5)$) which yield a comprehensive model of magnetic interactions in this material. Our main results are the following. (i) Isolated Cr^{3+} ion pairs in neighboring $4f_{vi}$ planes form singlets with a singlet-triplet splitting of 18.6(1) meV. These layers are only weakly coupled to a three-layer (111) pyrochlore slab which may also be described as two kagomé lattices separated by a triangular lattice. (ii) Cr^{3+} ions in these pyrochlore slabs reside on the vertices of corner-sharing tetrahedra, which form a highly frustrated quasi-two-dimensional magnet.

A powder sample of 50 g was prepared by a solid state reaction between stoichiometric amounts of Cr_2O_3, Ga_2O_3, and $SrCO_3$ in air at 1350 °C. We used high-temperature magnetic susceptibility data to determine the Cr^{3+} content in the sample to be $p = 0.92(5)$. We established the structure of our sample by measuring its neutron powder diffraction pattern using the 32 detector powder diffractometer BT1 at NIST. Starting from the magneto plumbite structure in space group $P6_3/mmc$, we used Rietveld refinement to extract the structural parameters listed in Table I. The parameters are consistent with the previously published structure [1], but occupancies of chromium, which are consistent with our determination from high-temperature susceptibility measurements, are somewhat higher.

The aspects of the crystal structure which are relevant for this paper are shown in Fig. 1. The magnetic Cr^{3+} ions occupy three distinct sites which are denoted $12k$, $2a$, and $4f_{vi}$, respectively. The $12k$ layer is a slightly distorted kagomé lattice, whereas the $2a$ and $4f_{vi}$ layers are triangular lattices. The Cr^{3+} ions in the $12k$-$2a$-$12k$ block form corner-sharing tetrahedra, as in three-layer (111) slabs of the trivalent cation sites in the cubic pyrochlore [8,9] and spinel structures. Each Cr^{3+} ion is surrounded by a distorted octahedron of oxygen atoms, for clarity, though, only selected oxygen atoms are shown in Fig. 1. Also excluded from the figure are triangular lattices of Sr($2d$) and Ga($2b$) which reside in between the $4f_{vi}$ chromium layers and two triangular Ga($4f_{iv}$) lattices which sandwich the $2a$ chromium layer. Neither of these nonmagnetic cation sublattices are expected to have a direct impact on magnetic exchange interactions.

Inelastic neutron scattering experiments were performed using the HET and MARI direct geometry spectrometers at the 160 kW ISIS pulsed spallation neutron source [10]. A Fermi chopper phased to the ≈ 1 μs, 50 Hz neutron pulses monochromates the incoming beam. We took our data with incident energies of 35 and 100 meV. On HET, banks of detectors cover the angular ranges of $\phi = 3°$ to $7°$ at a distance of 4 m from the sample and $\phi = 9°$ to $29°$ at a distance of 2.5 m. MARI detectors cover the angular range of $\phi = 2°$ to $\phi = 136°$ at a distance of 4 m. The angular

TABLE I. Positions within space group $P6_3/mmc$ and occupancies per formula unit (f.u.) of atoms in $SrCr_{9p}Ga_{12-9p}O_{19}$ at $T = 10$ K as determined by Rietveld analysis of the diffraction data displayed in Fig. 1 using the general structure analysis system [17]. The lattice parameters for the hexagonal unit cell at 10 K are $a = 5.7954(1)$ Å and $c = 22.6446(6)$ Å. Isotropic Debye-Waller factors, $\exp(-\langle u^2 \rangle Q^2)$, were used and the resulting overall reduced $\chi^2 = 2.0$.

Site	x	y	z	n/f.u.	$\sqrt{\langle u^2 \rangle}$/Å
Sr 2d	2/3	1/3	1/4	1	0.059(4)
Ga 2a	0	0	0	0.11(3)	0.039(5)
Cr 2a	0	0	0	0.89(3)	0.039(5)
Ga 2b	0	0	1/4	1	0.051(4)
Ga $4f_{iv}$	1/3	2/3	0.0276(1)	2	0.01(2)
Ga $4f_{vi}$	1/3	2/3	0.1908(2)	0.29(4)	0.039(5)
Cr $4f_{vi}$	1/3	2/3	0.1908(2)	1.71(4)	0.039(5)
Ga 12k	0.1687(4)	0.3374(8)	−0.1086(1)	0.59(8)	0.039(5)
Cr 12k	0.1687(4)	0.3374(8)	−0.1086(1)	5.41(8)	0.039(5)
O1 4e	0	0	0.1509(2)	2	0.02(1)
O2 4f	1/3	2/3	−0.0558(2)	2	0.047(4)
O3 6h	0.1811(3)	0.3621(7)	1/4	3	0.035(4)
O4 12k	0.1564(2)	0.3127(5)	0.0526(1)	6	0.020(6)
O5 12k	0.5047(3)	0.0094(5)	0.151 19(8)	6	0.040(3)

resolution is 0.6° for all detectors on both instruments. Scattering cross sections were normalized to within an accuracy of 20% by scaling magnetic scattering to nuclear Bragg peaks with a known scattering cross section.

Time-of-flight neutron spectrometers simultaneously collect scattering data over a range of energy and wavevector transfer. Figure 2 shows a color image of the normalized [11] intensity distribution, $I(Q, \omega)$, at $T = 1.5$ K. Apart from elastic nuclear scattering centered at $\hbar\omega = 0$ meV, $I(Q, \omega)$ is dominated by two ridges, one at fixed wave-vector transfer, $Q \approx 1.5$ Å^{-1}, and a most unusual ridge at fixed energy transfer $\hbar\omega = 18.6(1)$ meV. Since the constant-Q ridge covers a range of energies, $0 < \hbar\omega < 20$ meV, it must be associated with excitations in a system with a macroscopic number of interacting degrees of freedom. However, because the $\hbar\omega = 18.6$ meV ridge is narrow in energy and nondispersive (Figs. 2 and 3), it is likely to arise from single atoms or small clusters of atoms which are decoupled from the rest of the system. The constant-Q ridge corresponds to magnetic excitations in the frustrated spin system and was
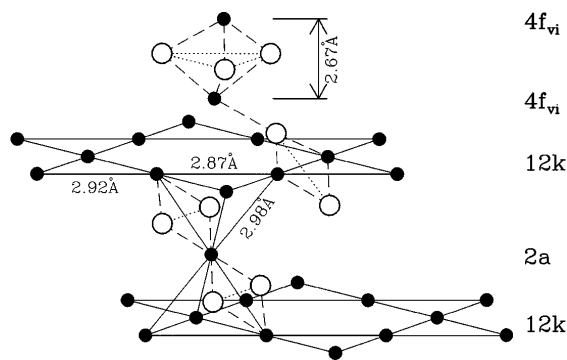
the subject of previous publications [3,6]. In this paper we shall deal exclusively with the excitations which give rise to the constant-$\hbar\omega$ ridge. From the Q dependence of the energy integrated intensity of the ridge [Fig. 3(c)], we conclude that it does not arise from (i) a local vibrational excitation, because the intensity decreases with Q, nor from (ii) a crystal field excitation on a single chromium atom because the Q dependence does not simply follow the magnetic form factor of chromium [12].

Further clues come from finite temperature properties. To enhance sensitivity we plot in Fig. 4 the Q-integrated intensity which probes the local spin fluctuation spectrum: $I(\omega) = \int [I(Q, \omega)/|F(Q)|^2] Q^2 \, dQ / \int Q^2 \, dQ$. We discover that at $T = 290$ K, the intensity found in the $\hbar\omega = 18.6$ meV peak at low T is distributed not only into a peak at $\hbar\omega = -18.6$ meV as required by detailed balance, but also into a well-defined peak at twice the energy, $\hbar\omega = 37.2(5)$ meV. There is also a temperature
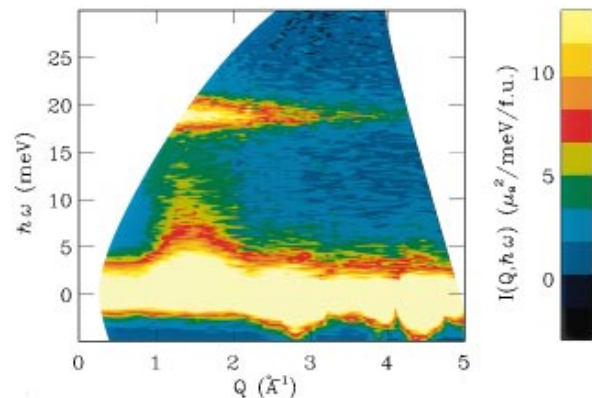

FIG. 1. Cr^{3+} sites in SCGO(p) (filled circles) and some of the oxygens atoms (open circles) which are part of their distorted octahedral coordination.

FIG. 2(color). Color image of normalized neutron scattering intensity, $I(Q, \omega)$, in SCGO($p = 0.92(5)$) at $T = 1.3$ K. The data were obtained in 1200 μA h of beam time on MARI with $E_i = 35$ meV using slit pack C rotating at 350 Hz.
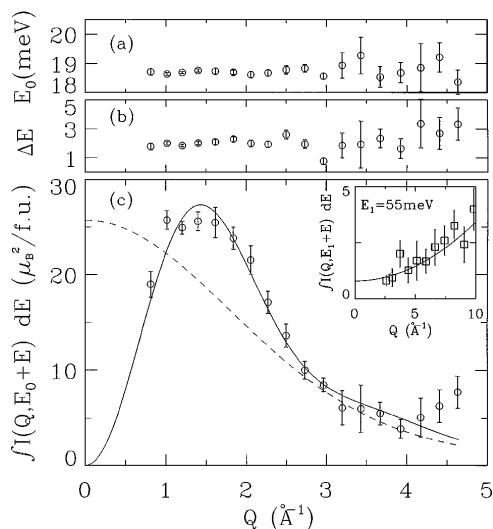
FIG. 3. Q dependence of inelastic scattering from nondispersive excitations in SCGO($p = 0.92(5)$) at $T = 1.3$ K as derived from Fig. 2. (a)–(c) The Q dependence of the peak position, resolution corrected FWHM, and integrated intensity, respectively, obtained from fits with Gaussians. In (c), the position and width of the peaks at each value of Q were fixed to the average obtained in individual fits. Dashed line in (c) shows the magnetic form factor of chromium, the solid line is the calculated Q dependence of the neutron scattering cross section in Eq. (1). The inset shows the Q dependence of the energy integrated intensity of the 55 meV peak which identifies this mode as vibrational in origin.

independent peak at $\hbar\omega \approx 55$ meV which is close to 3 times 18.6 meV. This peak, however, corresponds to a vibrational excitation because its integrated intensity increases with Q [inset in Fig. 3(c)]. Figure 5 summarizes the T dependence of the excitation energy, E_0, the resolution corrected full width at half maximum (FWHM), ΔE, of the 18.6 meV excitation, as well as the total scattering cross section for the 18.6 and 37.2 meV modes. These results were obtained by fitting data such as those in Fig. 4 with Gaussians. The fact that E_0 is T independent and $\Delta E/E_0 < 0.2$ even for $k_B T > E_0$ indicates that we are dealing with excitations between well-defined quantum states of isolated spin clusters relaxing through electron phonon coupling. The level scheme depicted in Fig. 5(c) assigns the 18.6 meV peak to transitions from the ground state to the first excited state at $J = 18.6$ meV and the 37.2 meV peak to transitions between excited states separated by $2J$. This model ensures that the latter peak is only observed at high T because only then does one of the excited states involved have finite thermal occupancy. From the absence of a peak of magnetic origin in $I(\omega)$ at $\hbar\omega = 3J = 55.8$ meV for $T < 290$ K we conclude that the $3J$ level is not dipolar active.

Pairs of spins, s, with antiferromagnetic exchange constant, J, have exactly this level scheme: Their states are labeled by their total spin quantum number, $S = 0, 1, 2, \ldots, 2s$, and lie at energies $JS(S + 1)/2$ relative to the ground state [13]. Moreover, only transitions which change S by one are dipolar active. To determine whether
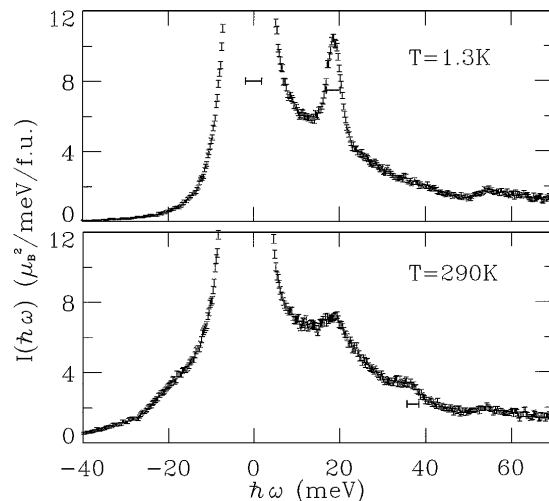

FIG. 4. ω dependence of the Q integrated neutron scattering intensity, $I(\omega) = \int[I(Q, \omega)/|F(Q)|^2]Q^2\, dQ / \int Q^2\, dQ$ in SCGO($p = 0.92(5)$) at $T = 1.3$ and 290 K. The data were obtained from 1139.3 μA h of beam time on HET with $E_i = 100$ meV using slit pack C rotating at 100 Hz. The horizontal bars show the FWHM of the instrumental resolution.

isolated spin pairs exist in SCGO(p) we perform a quantitative comparison of our data to the neutron scattering cross section for exchange coupled pairs of $s = 3/2$ Cr^{3+} ions in a powder sample [13,14],

$$\frac{d^2\sigma}{d\Omega\, dE'} = r_0^2 \frac{k'}{k} Nz \left\{\frac{1}{2} gF(Q)\right\}^2 \frac{1}{Z}\left(1 - \frac{\sin QR}{QR}\right)$$
$$\times\, [5\delta(\hbar\omega - J) + 8\exp(-J/k_B T)\delta(\hbar\omega - 2J)$$
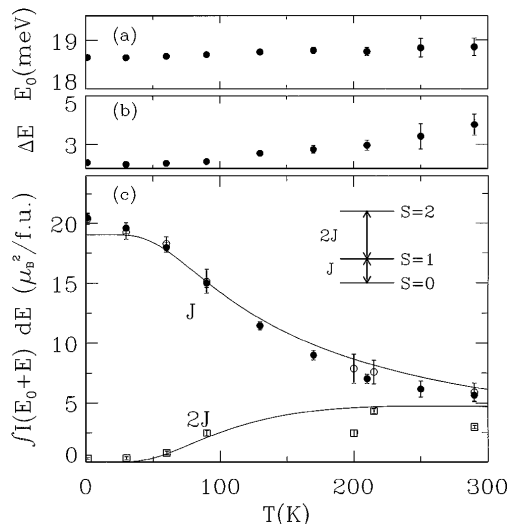$$+\, 7\exp(-3J/k_B T)\delta(\hbar\omega - 3J)], \quad (1)$$

FIG. 5. (a), (b) T dependence of the excitation energy and resolution corrected FWHM of the lowest energy inelastic peak in wave-vector integrated neutron scattering from SCGO($p = 0.92(5)$). (c) Q- and ω-integrated intensities of the 18.6 and the 37.2 meV excitations versus T. The solid lines were calculated from Eq. (1). The scattering data in this figure came from 6093.4 μA h of beam time on HET using $E_i = 35$ meV (filled circles) and $E_i = 100$ meV (open symbols) and slit pack C rotating at 300 and 100 Hz, respectively.

where R is the separation between spins in z spin pairs per formula unit and $Z = 1 + 3\exp(-J/k_BT) + 5\exp(-3J/k_BT) + 7\exp(-6J/k_BT)$ is the partition function. We write only the $\hbar\omega > 0$ part. The $\hbar\omega < 0$ part follows from detailed balance. There is also an elastic scattering term which appears when degenerate levels are occupied, but this is not relevant in this context.

The solid lines in Figs. 3(c) and 5(c) were calculated from this expression fitting only the distance between spins, R, and the number of spin pairs per formula unit, z. Both the Q dependence and T dependence of the intensity is perfectly accounted for by the model. Considering also the values of the fitting parameters, our data firmly establish the existence of $z = 0.7(1)$ spin pairs per formula unit in SCGO($p = 0.92(5)$) separated by $R \approx 2.68(7)$ Å with an antiferromagnetic exchange coupling $J = 18.6(1)$ meV. Since $4f_{vi}$ spins are the only spins which each are part of a unique spin pair and since according to our diffraction data there are 0.78 $4f_{vi}$-$4f_{vi}$ spin pairs per formula unit separated by 2.681(3) Å in our sample, we suggest that it is the $4f_{vi}$ Cr^{3+} ions which form the isolated spin pairs.

To justify this assignment, we must argue how $4f_{vi}$-$4f_{vi}$ spin pairs become effectively isolated from the remainder of the spins. Consider the oxygen coordination of chromium in SCGO(p). Each Cr^{3+} ion is surrounded by six oxygen atoms forming a distorted octahedron. Octahedra of chromium ions in adjacent $4f_{vi}$ planes share a common face, whereas the oxygen octahedra of neighboring $4f_{vi}$ and $12k$ sites share a corner. The exact same environment exists in corundum Cr_2O_3 where it has been established [15] that the exchange constant between Cr^{3+} ions with corner-sharing oxygen octahedra is only 0.2 meV because occupied $3d$ orbitals in Cr^{3+} do not hybridize with oxygen [16]. Occupied orbitals of Cr^{3+} ions in face-sharing octahedra, however, have appreciable direct overlap which in Cr_2O_3 gives rise to a 15 meV antiferromagnetic exchange coupling [15]. This number, being close to the 18.6 meV exchange constant for spin pairs in SCGO($p = 0.92(5)$), supports our comparison to Cr_2O_3 and our conclusion that $4f_{vi}$ spins pairs form isolated singlets in SCGO(p). The finite width of the excitations, which at $T = 1.3$ K amounts to $\Delta E/E_0 = 0.1$, most likely results from relaxation due to lattice vibrations and residual coupling to the remainder of the magnet.

Of course, the primary interest in SCGO(p) stems from its unusual frustrated magnetism. Our discovery that spins on $4f_{vi}$ sites are effectively isolated from those on $12k$ sites establishes that the spin system giving rise to low-temperature anomalies in this material is two dimensional, and consists of a triangular lattice ($2a$) sandwiched between two kagomé lattices ($12k$). Alternatively the lattice can be described as a three-layer (111) slab of the trivalent cation sites in the cubic pyrochlore lattice. The octahedra of all neighboring chromium ions in this slab share edges, and we therefore expect exchange interactions to be similar. Fitting high-temperature bulk susceptibility data to the

sum of the susceptibility of the $4f_{vi}$ spin pairs and a Curie-Weiss term to account for the pyrochlore slab, we extract a value of 9.0(5) meV for the average exchange constant within the pyrochlore slab. It is satisfying that this number is close to the value of 6.7(4) meV measured for the exchange constant between chromium ions in Cr_2O_3 whose oxygen octahedra share an edge [15]. Our discovery of the effective decoupling of different trilayer pyrochlore slabs in SCGO(p) should greatly simplify theoretical attempts to understand this unusual magnet.

We thank B. Judd for a useful discussion, Q. Huang and J. Stalick for their help in analyzing the diffraction data, E. Tesse and W. L. Chen for reading the manuscript, and the NSF for funding through Grants No. DMR-9302065, No. DMR-9453362, and No. DMR-9406115.

*Present addresses: University of Maryland, College Park, MD 20742 and National Institute of Standards and Technology, Gaithersburg, MD 20899.

[1] X. Obradors et al., Solid State Commun. **65**, 189 (1988).

[2] A. P. Ramirez et al., Phys. Rev. Lett. **64**, 2070 (1990); Phys. Rev. B **45**, 2505 (1992).

[3] C. Broholm et al., Phys. Rev. Lett. **65**, 3173 (1990); J. Magn. Magn. Mater. **69**, 4968 (1991).

[4] B. Martínez et al., Phys. Rev. B **46**, 10 786 (1992).

[5] Y. J. Uemura et al., Phys. Rev. Lett. **73**, 3306 (1994).

[6] S.-H. Lee, C. Broholm, G. Aeppli, A. P. Ramirez, T. G. Perring, C. J. Carlile, M. Adams, T. J. L. Jones, and B. Hessen (unpublished).

[7] D. A. Huse and A. D. Ruthenberg, Phys. Rev. B **45**, 7536 (1992); S. Sachdev, Phys. Rev. B **45**, 12 377 (1992); A. Chubukov, Phys. Rev. Lett. **69**, 832 (1992); D. L. Huber and W. Y. Ching, Phys. Rev. B **47**, 3220 (1993); I. Ritchey et al., Phys. Rev. B **47**, 15 342 (1993); E. F. Shender et al., Phys. Rev. Lett. **70**, 3812 (1993); P. Chandra et al., J. Phys. I (France) **3**, 591 (1993); J. N. Reimers and A. J. Berlinsky, Phys. Rev. B **48**, 9539 (1993).

[8] M. J. Harris et al., Phys. Rev. Lett. **73**, 189 (1994).

[9] J. N. Reimers et al., Phys. Rev. B **43**, 3387 (1991); J. E. Greedan et al., Phys. Rev. B **43**, 5682 (1991).

[10] B. Boland and S. Whapham, "Users Guide to Experimental Facilities at ISIS," RAL 92-041 (1992).

[11] $I(Q,\omega)$ is related to the double differential neutron scattering cross section [14] by $I(Q,\omega) = (1/N) \times (2\mu_B/r_0)^2(k/k')d^2\sigma/d\Omega\, dE'$, where N is the number of formula units in the sample and $r_0 = 0.54 \times 10^{-12}$ cm.

[12] A. J. Freeman and R. E. Watson, Acta Cryst. **14**, 231 (1961).

[13] A. Furrer and H. U. Güdel, J. Magn. Magn. Mater. **14**, 256 (1979).

[14] We use the notation of S. W. Lovesey, *Theory of Neutron Scattering from Condensed Matter* (Clarendon Press, Oxford, 1984). Note that for a single crystalline sample where spherical averaging does not occur, $\sin QR/QR$ should be replaced by $\cos \mathbf{Q} \cdot \mathbf{R}$ in Eq. (1).

[15] E. J. Samuelsen et al., Physica **48**, 13 (1970).

[16] J. B. Goodenough, Phys. Rev. **117**, 1442 (1960).

[17] A. C. Larson and R. B. Von Dreele, Los Alamos National Laboratory Report No. LAUR 86-748.